ELSEVIER

Journal of Photochemistry and Photobiology A: Chemistry 97 (1996) 11–18

Journal of PHOTOCHEMISTRY AND PHOTOBIOLOGY A:CHEMISTRY

Aromatic ketones as standards for singlet molecular oxygen $O_2(^1\Delta_g)$ photosensitization. Time-resolved photoacoustic and near-IR emission studies [1,2]

Cristina Martí, Oriol Jürgens, Oriol Cuenca, Mercè Casals, Santi Nonell *

CETS Institut Químic de Sarrià, Universitat Ramon Llull, Via Augusta 390, 08017-Barcelona, Spain

Received 29 November 1995; accepted 20 January 1996

Abstract

Time-resolved near-IR emission and optoacoustic calorimetry studies were carried out on the aromatic ketones phenalenone, benzanthrone, 4-phenylbenzophenone and the benzophenone–naphthalene (0.1 M) system in order to assess their adoption as solvent-independent standards for singlet molecular oxygen $O_2(^1\Delta_g)$ photosensitization. All compounds show quantum yields of $O_2(^1\Delta_g)$ production (ϕ_Δ) in the range 0.9–1 in cyclohexane. Increasing solvent polarity or protic character reduces the ϕ_Δ values for all sensitizers except phenalenone. Laser-induced optoacoustic calorimetry was used to obtain the absolute ϕ_Δ values for the latter compound by applying both maximum amplitude and deconvolution methods. The former yields highly precise results (3%–5% uncertainty) and has been chosen for standardization purposes. The deconvolution method yields both kinetic and quantum yield data, albeit with lower precision (10%–15% uncertainty).

Keywords: Aromatic ketone; Photosensitization; Singlet molecular oxygen; Standard

1. Introduction

Photo-oxygenation processes mediated by singlet molecular oxygen $O_2(^1\Delta_g)$ continue to attract the attention of the scientific community owing to their application in various areas, such as the synthesis of novel compounds, purification of wastewaters, photodegradation of polymers and photodynamic therapy of different diseases. For a large number of compounds, considerable efforts have been devoted to the quantification of the ability to act as $O_2(^1\Delta_g)$ photosensitizers. Recently, a compilation of $O_2(^1\Delta_g)$ production quantum yields (ϕ_Δ) has been published [1]. Data originating in different laboratories on a given compound show a high degree of scatter. In most cases, this scatter can be traced to real differences in the system variables, e.g. solvent, temperature, excitation wavelength, etc. In others, however, the scatter originates from the method of measurement.

Quantum yields of $O_2(^1\Delta_g)$ production can be measured by optical, chemical and calorimetric methods. Of these, the methods of choice are those involving optical techniques as these directly monitor $O_2(^1\Delta_g)$. Optical methods are based on the comparison between the $O_2(^1\Delta_g)$ phosphorescence in the near-IR region (1270 nm) produced by a sample and a reference sensitizer, i.e. a substance whose ϕ_Δ value is known with accuracy under the experimental conditions used. Establishing standards is therefore of prime interest. The comparison requires, among other conditions, that the sample and reference sensitizer are dissolved in the same solvent, as the $O_2(^1\Delta_g)$ radiative rate constant is dramatically solvent dependent [2,3]. This requirement is far more demanding than in conventional fluorescence spectroscopy and, as a consequence, a reference is needed for every possible solvent.

The most common approach to the determination of absolute ϕ_Δ values is the use of chemical methods that trap $O_2(^1\Delta_g)$ with reactive substrates. They are indirect, as the quantity actually measured is the extent of substrate depletion, oxygen consumption or reaction product build-up [1]. The specificity of the substrate towards $O_2(^1\Delta_g)$ is an inherent problem and source of uncertainty, as other mechanisms may be involved in the photo- oxygenation process. Furthermore, the relative contribution of the different mechanisms is strongly solvent dependent, a complication which hampers the use of a given acceptor in a wide range of solvents.

An alternative approach is the use of calorimetric methods, e.g. laser-induced optoacoustic calorimetry (LIOAC), time-

[1] Dedicated to Professor Lluís Victori on the occasion of his 60th birthday.

[2] This work was presented at the 6th Congress of the European Society for Photobiology, Cambridge, 1995.

* Corresponding author.

PII S1010-6030(96)04321-3

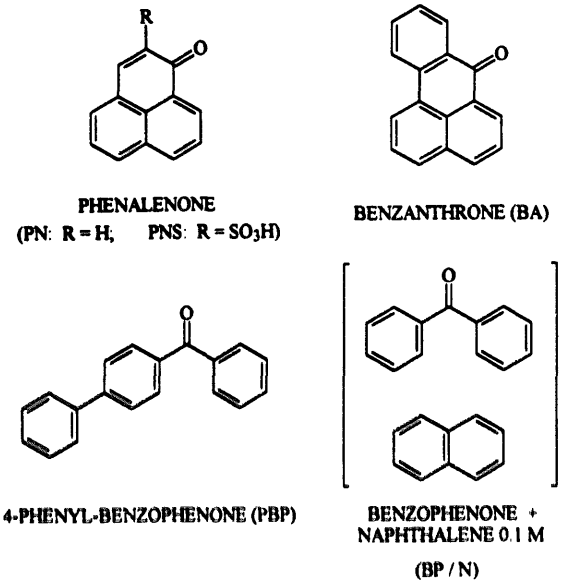

Scheme 1. Chemical structures of the sensitizers studied in this work.

resolved thermal lensing (TRTL) or the more sophisticated photothermal beam deflection (PBD), which monitor the radiationless processes concomitant with $O_2(^1\Delta_g)$ production and decay [4–7]. They are especially well suited for $O_2(^1\Delta_g)$ detection since most of the energy of this species is lost through non-radiative channels. Calorimetric methods are also comparative, the photocalorimetric reference being a substance which releases all absorbed energy as heat on a time scale much shorter than the time window of the experiment [8]. Although sample and reference still need to be measured in the same solvent (the signal intensity depends on its thermoelastic properties [8]), calorimetric methods have a clear advantage over chemical and optical techniques since universal solvent-independent photocalorimetric references are widely available. They are therefore free from the uncertainties associated with solvent changes. Although TRTL has been successfully applied to the determination of ϕ_Δ for several sensitizers, including aromatic hydrocarbons and ketones, the use of the experimentally less demanding LIOAC has been limited to a few sensitizers [6,7,9,10]. In this work, the suitability and limitations of the LIOAC technique for the determination of ϕ_Δ values are studied.

Of the compounds known to photosensitize effectively the formation of $O_2(^1\Delta_g)$, aromatic ketones are interesting as potential standards as they often have intersystem crossing quantum yields close to unity, i.e. only triplet state reactions need to be considered when discussing their photochemistry. Energy transfer to oxygen to form singlet oxygen largely dominates (efficiency close to unity) when the ketone's lowest triplet state is of ($\pi\pi^*$) configuration [11,12]. A number of research groups have used such aromatic ketones for $O_2(^1\Delta_g)$ photosensitization, e.g. 4-phenyl-benzophenone (PBP) [13], benzanthrone (BA) [14], phenalenone (PN) [9,13,15] and its water-soluble 2-sulphonic acid derivative (PNS) [16] and the elegant system of an aromatic ketone, e.g. benzophenone, plus naphthalene (0.1 M) (BP–N; Scheme 1) [17–19]. Both phenalenone and the aromatic ketone–naphthalene (0.1 M) system have been reported to have ϕ_Δ values close to unity in solvents of various polarities [9,15,17–19]. However, Wilkinson et al. [20] obtained somewhat lower solvent-dependent values for the BP–N system. PN seems to be free from such drawbacks: the original work of Oliveros et al. [15] reporting $\phi_\Delta = 0.93$ in benzene and $\phi_\Delta = 0.97$ in deuterated methanol has been extended by Schmidt et al. [9] to several solvents. Their results suggest an average ϕ_Δ value of 0.95 ± 0.05 in most solvents. In the hope of contributing to the adoption of PN as a general standard, we report data on this compound using alternative methods and techniques. In addition, we report the solvent dependence of ϕ_Δ for the other ketones BA, PBP and the BP–N system, studied to assess their use as alternative standards.

2. Materials and methods

2.1. Chemicals

PN, PBP, BA, BP, 2-hydroxy-benzophenone (2HBP), ferrocene (FC) and bromocresol purple (BCP) were purchased from Aldrich. Analytical grade anthracene was from Merck. All were used as received. Naphthalene was purchased from Panreac and recrystallized prior to use. PNS was prepared as described previously [16]. All solvents, purchased from SDS, were of HPLC or spectroscopic grade, and were used without further treatment. Argon and oxygen from Carburos Metálicos were of purity better than 99.99%. For oxygen quenching experiments, they were mixed to the desired proportion using calibrated flow meters, the oxygen concentration in the solutions being calculated using published solubility data after correcting for the vapour pressure of the solvent [21,22]. Specifically, vapour pressures at 25 °C were taken as: cyclohexane, 97.8 Torr; toluene, 28.5 Torr; acetonitrile, 88.8 Torr; ethanol, 59.0 Torr; dichloromethane, 435.8 Torr; for D_2O the value in H_2O was taken, 23.8 Torr. The oxygen solubility values at 1 atm O_2 partial pressure were taken as: cyclohexane, 11.5 mM; toluene, 9.88 mM; acetonitrile, 9.1 mM; ethanol, 9.92 mM; dichloromethane, 10.7 mM; for D_2O the value in H_2O was taken, 1.27 mM.

2.2. Methods

Absorption spectra were measured with a Varian Cary 4E or a Perkin Elmer Lambda 2 spectrophotometer, periodically calibrated with a holmium oxide filter (Hellma). Fluorescence spectra were measured with a Shimadzu RF-540 spectrofluorometer. Fluorescence quantum yields were determined following standard procedures using anthracene in ethanol or naphthalene in cyclohexane as standards [23].

The laser facility for $O_2(^1\Delta_g)$ phosphorescence detection (TRPD) is based on that described previously [24,25]. An N_2 laser (Radiant Dyes Laser Accessories) delivering 5 mJ,

6 ns pulses at 337 nm was used to excite air-saturated samples contained in a 1 cm path length quartz cuvette. The diameter of the beam in the cuvette was reduced to approximately 8 mm by a 100 cm lens. The laser fluence was varied using a variable neutral density filter and measured by diverting a small fraction of the beam onto a pyroelectric energy meter (Laser Precision Corp. RJ7610 with RJP-735 head) by means of a calibrated beam splitter. The luminescence arising from the cuvette was passed through a 1050 nm cut-off silicon filter and a 1270 nm interference filter, and detected with a bias-reversed 5 mm diameter Judson J16 5Sp germanium diode (time response, 600 ns). After amplification with a home-built amplifier, the signal was fed to a 150 MHz Lecroy 9410 digital oscilloscope for digitizing and averaging (typically 100 shots), and finally transferred to a PC by means of a National Instruments AT-GPIB interface and LabWindows software. The trigger signal for the scope was provided by an auxiliary fast photodiode detecting yet another small diverted fraction of the beam. In all solvents and for all laser fluences, the decay portion of the signals could be fitted with a single-exponential function, whose zero time intensity $S(0)$ is related to ϕ_Δ through

$$S(0) = \kappa k_R \phi_\Delta E_l (1 - 10^{-A}) \quad (1)$$

where κ is a proportionality constant that includes geometric and electronic factors of the detection system, k_R is the solvent-specific radiative decay rate constant, E_l is the incident laser energy and A is the sample absorbance at 337 nm. While, in principle, the ϕ_Δ values can be determined from the simple comparison of $S(0)$ for sample and reference under the same E_l and A conditions, greater accuracy is obtained when $S(0)$ is measured as a function of E_l keeping A constant. The observation of a linear relationship with zero intercept permits undesirable phenomena such as multiphotonic absorption or ground state depletion to be ruled out. Repetition of these experiments at several absorbances, each yielding a linear $S(0)$ vs. E_l plot with slope $(\partial S(0)/\partial E_l)_A$, allows the construction of a slope vs. $(1 - 10^{-A})$ plot for both sample and reference. This eliminates the uncertainties associated with the exact matching of the absorbance for sample and reference. The ratio of the slopes for these plots ultimately affords the ratio of the ϕ_Δ values.

LIOAC uses a piezoelectric transducer to sense the pressure wave concomitant with local volume changes induced by pulsed laser irradiation of the sample. Volume changes can have a thermal origin, i.e. heating of the solvent through excited state radiationless decay processes or secondary chemical reactions [8,26–30], and sometimes a structural origin, e.g. as a result of a chemical reaction or solvent reorganization [31–34]. The set-up used is essentially identical with that for TRPD except for the laser beam geometry and the detection system. We tried both a 1 mm diameter circular beam produced by a 100 cm lens in combination with a 1 mm aperture [35] and a rectangular 1 mm × 8 mm beam produced by a 100 cm cylindrical lens plus a 100 cm lens and a 1 mm vertical slit [36]. The results using both geometries were the same, but the slit produced a fivefold better signal-to-noise ratio. The solutions were contained in a standard gas-tight 1 cm × 1 cm quartz cuvette and the pressure wave was detected with a 4 mm PZT ceramic transducer (Vernitron; 1 MHz) pressed to the side wall of the cuvette. A thin layer of silicon grease ensured optimum acoustic coupling between the cuvette and transducer. This detection system is similar to that described by Patel and Tam [26] and was assembled at the Max-Planck-Institut für Strahlenchemie [35]. Extreme care was taken not to disturb this coupling during a series of experiments. The signals were fed to the scope and transferred to a PC. Analysis was accomplished following two different approaches. The first takes the intensity of the optoacoustic signal maximum as a measure of the volume changes [26,35]. The second is based on the deconvolution of the pressure–time waveform [6,37–39].

2.2.1. LIOAC determinations with the maximum amplitude method

The amplitude of the first signal maximum H_{max} was calculated from the best second-order polynomial fit to the data points near the maximum. In the absence of structural volume changes, the optoacoustic maximum amplitude H_{max} is related to the incident laser energy by

$$H_{max} = \kappa' \alpha E_l (1 - 10^{-A}) \quad (2)$$

where κ' is a proportionality constant that accounts for geometric and electronic factors, as well as for the thermoelastic properties of the solvent, and α is the fraction of absorbed energy released as fast heat. The attribute "fast" is related to the effective acoustic transient time ($\tau'_a = d/v_a$, where d is the beam diameter and v_a is the sound velocity in the solvent used; in our experiments $\tau'_a \approx 1$ μs) [8]. The transducer integrates the heat deposited in processes faster than roughly $\tau'_a/5$ and ignores all processes slower than $5\tau'_a$ [40]. The intermediate cases are discussed below. The α value is obtained by the systematic measurement of H_{max} as a function of E_l and A for both sample and reference, as described for TRPD. We used 2HBP and FC as calorimetric references ($\alpha = 1$) for organic media, and BCP for water [41,42]. Thus $\alpha < 1$ indicates that an energy-storing species living longer than $5\tau'_a$ is produced in the system. An energy balance permits α to be related to the energy content of this species

$$E_\lambda = \alpha E_\lambda + \phi_f E_f + \phi_{st} E_{st} \quad (3)$$

where E_λ, E_f and E_{st} are the molar energy contents of the laser photons (356 kJ mol^{-1} for the N_2 laser), fluorescence photons and long-lived species respectively, and ϕ_f and ϕ_{st} are the quantum yields of fluorescence and production of the energy-storing species respectively. For our ketones, dissipation through radiative processes is negligible (see Section 3). In argon-saturated solutions, the storing species is the sensitizer's triplet state whose lifetime spans several tens of microseconds [15]. Assuming $\phi_{isc} = 1$, E_T is calculated from the measured α value as $E_T = E_\lambda(1 - \alpha)$. In the presence of oxygen, the storing species is $O_2(^1\Delta_g)$ whose energy content

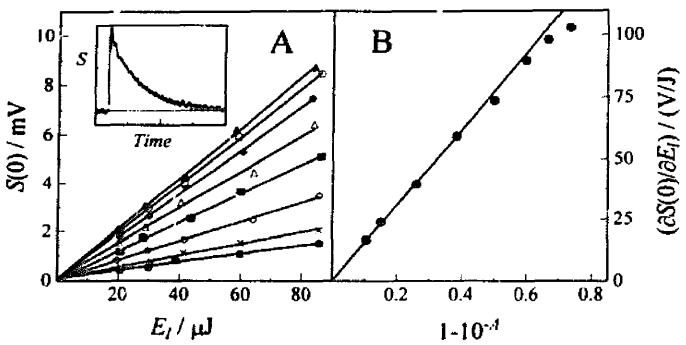

Fig. 1. (A) Laser energy dependence of the zero time intensity of the $O_2(^1\Delta_g)$ phosphorescence signal sensitized by BA in cyclohexane. Inset: typical $O_2(^1\Delta_g)$ phosphorescence rise and decay. (B) Slopes of the energy plots as a function of the sample absorbance.

is $E_\Delta = 94.2$ kJ mol^{-1}. In this case, ϕ_Δ values are calculated as $\phi_\Delta = (1-\alpha)E_A/E_\Delta = 3.77(1-\alpha)$.

2.2.2. LIOAC determinations with the deconvolution method

For systems in which (1) the laser pulse duration is much shorter than the excited state lifetime and the detector response time, (2) and the structural volume changes are negligible, the observed energy-normalized optoacoustic wave $S(t)$ is a convolution of the system response $R(t)$ and the rate of heat evolution $q'(t)$ as shown in Eq. (4) [36–39]

$$S(t) = H(t)/E_I(1-10^{-A}) = R(t) \otimes q'(t) = \int_0^t R(t)q'(t-u)\,du \quad (4)$$

where $H(t)$ is the observed waveform. For short-lived transients, this integral approaches $R(t)$, the system response. Hence $R(t)$ can be experimentally determined by measuring a calorimetric reference. At the opposite extreme are those transients living longer than approximately $5\tau'_a$. The convolution integral now vanishes to zero, i.e. slow transients do not contribute to the optoacoustic signal. For systems in which only "fast" and "slow" processes occur, the observed wave is identical in shape to $R(t)$, but has a smaller amplitude. The undetected heat corresponds to the "stored" heat in the maximum amplitude method discussed above, whose use under these conditions is therefore legitimate. The deconvolution method is best suited for treating intermediate cases, where a clear phase shift between $S(t)$ and $R(t)$ exists. A kinetic decay model $q_{calc}(t)$ is assumed and the parameters are optimized for the calculated convolution $C(t) = R(t) \otimes q'_{calc}(t)$ to reproduce in the best way the observed waveform $S(t)$. The deconvolution by iterative reconvolution program used is based on the Lavenberg–Marquardt χ^2 minimization procedure [39].

3. Results and discussion

3.1. Fluorescence quantum yields

All compounds are essentially non-fluorescent in aprotic solvents ($\phi_f < 10^{-4}$), but a weak fluorescence is observed in ethanol for both BA ($\phi_f = 1.3\times10^{-3}$) and PBP ($\phi_f = 5\times10^{-3}$), probably reflecting a reordering of the singlet and triplet ($\pi\pi^*$) and ($n\pi^*$) energy levels [43–46]. In any case, the fluorescence yields are so low that radiative deactivation can safely be neglected in the analysis of LIOAC experiments (see below).

3.2. Relative ϕ_Δ values from TRPD experiments

Fig. 1 shows the energy dependence plots, and absorbance dependence of their slopes, for BA in cyclohexane. Similar plots were obtained for all sensitizers in all solvents. The values of ϕ_Δ relative to that of PN are collected in Table 1. Clearly, PN emerges as the most efficient sensitizer in all solvents, with the exception perhaps of BA in non-polar cyclohexane and toluene. It is also apparent that the other ketones have ϕ_Δ values close to unity in non-polar solvents only, yielding significantly lower values as the medium polarity or protic character increases.

The solvent dependence of the ϕ_Δ values rules out BA, PBP and BP–N as universal standards. This conclusion is particularly relevant for the aromatic ketone–naphthalene system, which had been suggested as a valuable standard with ϕ_Δ close to unity in cyclohexane and acetonitrile [17–19]. Our results (cf. Table 1) are in line with those reported by Wilkinson et al. [20], e.g. $\phi_\Delta = 0.92$ in cyclohexane and $\phi_\Delta = 0.62$ in acetonitrile.

Table 1
Solvent dependence of the relative ϕ_Δ values for the sensitizers studied as determined by TRPD

Sensitizer	Relative ϕ_Δ value [a]				
	Cyclohexane	Toluene	Acetonitrile	Ethanol	Dichloromethane
PN	1	1	1	1	1
BA	1.03	1.03	0.78	0.81	0.81
PBP	0.92	0.96	0.83	0.83	0.83
BP–N	1.00	0.82	0.65	0.79	0.79

[a] ±5%.

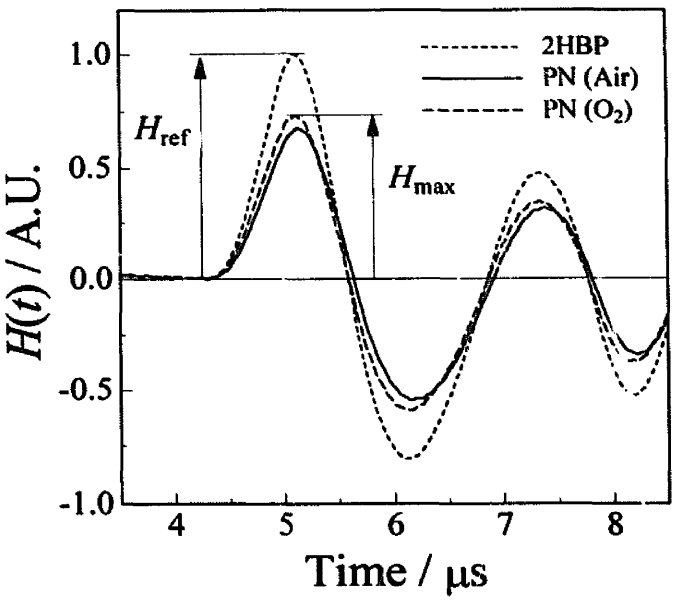

Fig. 2. Oxygen concentration effects on the PN optoacoustic wave in ace tonitrile solutions. The reference wave was obtained using 2HBP.

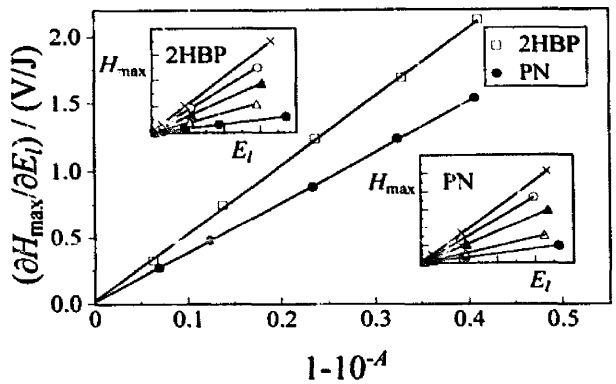

Fig. 3. Slopes of the optoacoustic maximum amplitude vs. laser energy plots as a function of the sample absorbance for PN and 2HBP in acetonitrile. Insets: laser energy dependence of the optoacoustic maximum amplitude for PN and 2HBP at several absorbances.

3.3. Absolute ϕ_Δ values for PN from LIOAC

TRPD experiments pointed to PN as the most promising standard candidate of the ketones studied in this work. As a next step, we undertook the determination of the absolute ϕ_Δ value for this compound using LIOAC. In this process, we explored and compared the maximum amplitude and deconvolution methods.

3.3.1. Maximum amplitude method

Fig. 2 shows typical LIOAC waveforms for air- and oxygen-saturated MeCN solutions of PN and the calorimetric reference 2HBP. Clearly, the sensitizer wave is phase shifted with respect to that of the reference under air-saturated conditions, an indication that the energy transfer step from the ketone triplet to oxygen occurs in the intermediate $\tau'_a/5 \leqslant \tau \leqslant 5\tau'_a$ region, where the amplitude wave is no longer proportional to the heat released. Analysis of the amplitude ratio α using Eq. (3) was not attempted as it would yield apparent ϕ_Δ values larger than the true values.

When air was replaced by oxygen, the shift was no longer present and the maximum amplitude increased as anticipated (cf. Fig. 2). The same was true for all other solvents, with the exception of CH_2Cl_2 and D_2O, where the concentration of oxygen was lower. In D_2O, where PNS and BCP were used instead of the less soluble PN and 2HBP, this is due to the low solubility of oxygen, assumed to be the same as in H_2O [22]. In CH_2Cl_2, this is the result of a relatively large solvent vapour pressure [21]. Fig. 3 shows the energy and absorbance dependence plots in acetonitrile. Similar plots were obtained in all solvents, and the ϕ_Δ results, calculated using Eq. (3), are collected in Table 2. It is remarkable that the error bars do not exceed 3%–5%.

The case of toluene deserves special comment. Toluene forms a charge transfer complex with oxygen whose absorbance at 337 nm is comparable with that of the sensitizer ($A_{tolO2} = 0.063$ under oxygen), i.e. this complex effectively competes with the sensitizer for light absorption. Furthermore, excitation of the toluene–oxygen complex produces

Table 2
Absolute quantum yields for $O_2(^1\Delta_g)$ photosensitization (ϕ_Δ), triplet energies (E_T), triplet lifetimes in air-saturated solutions (τ_T(air)) and rate constants for triplet quenching by oxygen ($k_{T\Sigma}$) for PN in several solvents (PNS in water), as determined by LIOAC using the maximum amplitude and deconvolution methods

Solvent	ϕ_Δ		E_T (kJ mol^{-1})		τ_T(air) (μs)	$k_{T\Sigma}$ (10^9 M^{-1} s^{-1})
	Maximum amplitude	Deconvolution	Maximum amplitude	Deconvolution		
Cyclohexane	0.91 ± 0.03	0.98 ± 0.08	174 ± 5	166 ± 22	260 ± 90	2.9 ± 0.2
Toluene	0.92 ± 0.03		178 ± 8			2.2 [d]
Dichloromethane	– [a]	0.96 ± 0.08	183 ± 8	180 ± 4	470 ± 20	1.9 ± 0.2
Acetonitrile	1.00 ± 0.02	0.94 ± 0.08	182 ± 10	164 ± 12	230 ± 40	3.2 ± 0.2
Ethanol	0.92 ± 0.03	0.93 ± 0.08	182 ± 8	176 ± 11	250 ± 20	2.9 ± 0.2
Water (PNS)	– [a]	0.97 ± 0.06 [b]	168 ± 10 [c]	180 ± 4 [b]	1700 ± 200 [b]	1.3 ± 0.1 [b]

[a] The method cannot be applied (see text).
[b] In D_2O.
[c] In H_2O.
[d] Ref. [13].

Process	Model Heat Function $q_{calc}(t)$
$^1M_0 \xrightarrow{h\nu} {}^1M_a$	---
$^1M_a \xrightarrow{fast} {}^1M_1 \xrightarrow{k_S} {}^3M_1$	$\frac{(E_\lambda - E_T)}{E_\lambda} \cdot (1 - e^{-k_S t})$
$^1M_1 + O_2(^3\Sigma_g^-) \xrightarrow{k_T}$ $^1M_0 + O_2(^1\Delta_g)$	$\frac{\phi_\Delta \cdot (E_T - E_\Delta)}{E_\lambda} \cdot (1 - e^{-k_T t})$
$^1M_0 + O_2(^1\Sigma_g^-)$	$\frac{(1-\phi_\Delta) \cdot E_T}{E_\lambda} \cdot (1 - e^{-k_T t})$
$O_2(^1\Delta_g) \xrightarrow{k_\Delta} O_2(^3\Sigma_g^-)$	$\frac{\phi_\Delta \cdot E_\Delta}{E_\lambda} \cdot (1 - e^{-k_\Delta t})$

Scheme 2. Kinetic and calorimetric analysis of the excited state behaviour of the sensitizers. It is assumed that the triplet quantum yield is close to unity and that triplet decay occurs exclusively through oxygen quenching in air- and oxygen-saturated solutions ($k_T \approx k_{T\Sigma}[O_2]$; see text).

$O_2(^1\Delta_g)$ with $\phi_\Delta = 0.2$ [47]. Thus the measured α value is actually a combination of the respective values for PN and the charge transfer complex as shown in Eq. (5)

$$\alpha = \frac{\alpha_{tolO_2} A_{tolO_2} + \alpha_{PN} A_{PN}}{A_{tolO_2} + A_{PN}} \quad (5)$$

From the measured α value and the calculated α_{tolO_2} value (0.95 for 337 nm excitation, using Eq. (3)), the true α_{PN} value is readily determined. The resulting $\phi_\Delta = 0.92$ is in very good agreement with that reported by Oliveros et al. [15] in benzene, $\phi_\Delta = 0.93$.

3.3.2. Deconvolution method

For $O_2(^1\Delta_g)$ sensitization by the ketones used here in the presence of enough oxygen to trap most triplet sensitizers, the heat release dynamics can be modelled with the simplified kinetic treatment shown in Scheme 2 [33] where k_S, k_T and k_Δ are the observed unimolecular or pseudo-unimolecular decay rate constants for $^1M_1$, $^3M_1$ and $O_2(^1\Delta_g)$ respectively. It is implicit in the heat functions that the three processes, i.e. triplet state formation, triplet quenching by oxygen and $O_2(^1\Delta_g)$ decay, occur on different time scales, i.e. $k_S \gg k_T \gg k_\Delta$. The total model heat function is then the sum of the above terms (Eq. (6))

$$q_{calc}(t) = \frac{E_\lambda - E_T}{E_\lambda}(1 - e^{-k_S t}) + \frac{E_T - \phi_\Delta E_\Delta}{E_\lambda} \times (1 - e^{-k_T t}) + \frac{\phi_\Delta E_\Delta}{E_\lambda}(1 - e^{-k_\Delta t}) \quad (6)$$

and the convolution of its time derivative with $R(t)$ renders

$$C(t) = R(t) \otimes (\alpha_1 k_S e^{-k_S t} + \alpha_2 k_T e^{-k_T t}) \quad (7)$$

where $\alpha_1 = (E_\lambda - E_T)/E_\lambda$ and $\alpha_2 = (E_T - \phi_\Delta E_\Delta)/E_\lambda$. The deconvolution procedure allows for the estimation of α_1 and α_2 (hence E_T and ϕ_Δ), as well as k_S and k_T, in a single experiment. While this is definitely an advantage over the more tedious maximum amplitude method, the results have larger error bars. This stems from the requirement that sample and reference must be measured under exactly the same conditions, i.e. matched absorbances and identical laser energies, thereby precluding the construction of the linear trends in laser energy and absorbance as in the maximum amplitude method (see above). It is certainly possible, in principle, to obtain an energy-normalized average waveform from such trends, but our experience is that the deconvolution of these average waveforms yields highly scattered results. We found that the best procedure was to repeat the measurements for sample and reference at fixed absorbance and laser energy (typically 16 times), and to report the average and standard deviation of such repetitions. The amplitude of the optoacoustic waveform was previously checked for linearity in laser energy and sample absorption. Fig. 4 shows the PN and 2HBP waves in air-saturated CH_2Cl_2, the best-fit convoluted wave calculated using Eq. (7) and the fit residuals. The results are also collected in Table 2 and are in good agreement with those obtained by the maximum amplitude method, except for the aforementioned larger uncertainties.

3.4. Oxygen quenching of PN triplet state

The triplet lifetime data determined by the deconvolution method can be used to deduce the rate constant for triplet quenching by oxygen according to the Stern–Volmer equation

$$k_T = 1/\tau_T = k_T^0 + k_{T\Sigma}[O_2] \quad (8)$$

A series of experiments was carried out in which τ_T in PN solutions saturated with mixtures of argon and oxygen was

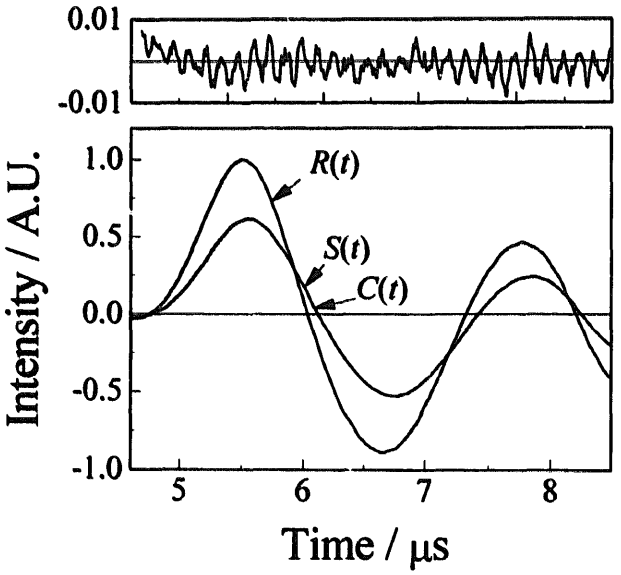

Fig. 4. LIOAC waveforms for PN and 2HBP in air-saturated CH_2Cl_2 ($S(t)$ and $R(t)$ respectively), best-fit convolution according to Eq. (7) ($C(t)$) and residuals of the fit.

Table 3
Recommended absolute ϕ_Δ values for the sensitizers studied in this work

Sensitizer	Absolute ϕ_Δ values					
	Cyclohexane	Toluene	Acetonitrile	Ethanol	Dichloromethane	Water-d_2
PN [a]	0.91 ± 0.03	0.92 ± 0.03	1.00 ± 0.03	0.92 ± 0.03	0.96 ± 0.08	-
PNS [a]	-	-	-	-	-	0.97 ± 0.06
BA [b]	0.94 ± 0.07	0.95 ± 0.07	0.78 ± 0.06	0.75 ± 0.06	0.78 ± 0.06	-
PBP [b]	0.84 ± 0.06	0.88 ± 0.06	0.83 ± 0.06	0.76 ± 0.06	0.80 ± 0.06	-
BP-N [b]	0.91 ± 0.07	0.75 ± 0.06	0.65 ± 0.05	0.73 ± 0.06	0.76 ± 0.06	-

[a] From LIOAC experiments.
[b] From TRPD experiments using PN as standard (see Table 1).

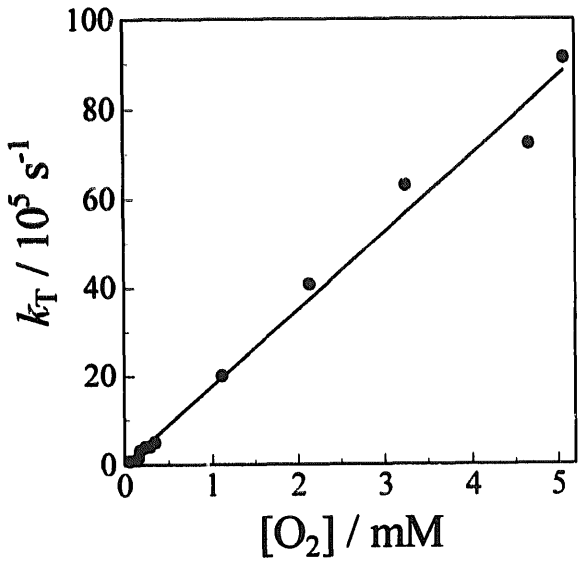

Fig. 5. Stern–Volmer plot for triplet PN quenching by oxygen in CH_2Cl_2 using τ_T values determined by LIOAC.

determined using the LIOAC deconvolution technique. Fig. 5 shows the Stern–Volmer plot obtained in CH_2Cl_2. From the slope, the quenching rate constant can be obtained and is shown in Table 2, together with the values for the other solvents. Although it is possible, in principle, to obtain the triplet lifetime at zero oxygen concentration, $\tau_T^0 = 1/k_T^0$, from such plots, the error bars of the intercept are too large to provide a good estimate. Thus all plots had an intercept indistinguishable from zero within experimental error, which is in agreement with the flash photolysis data on τ_T^0, e.g. $\tau_T^0 = 38$ μs in benzene [15]. The quenching rate constants obtained are in the $(1.3–3.2) \times 10^9$ M^{-1} s^{-1} range, close to one-ninth of the diffusional value [12,13,48,49]. This result is consistent with a triplet energy value lower than 200 kJ mol^{-1}, as first pointed out by Gijzeman et al. [50,51] and recently observed for a series of substituted naphthalenes [20].

3.5. Triplet state energy for PN

As a further check of the above results, we also determined the E_T values by applying the more precise maximum amplitude method to argon-saturated solutions of PN. The maximum amplitude method is especially well suited for the determination of the triplet state energy in this case since, in the absence of oxygen, the long-lived triplet state acts as the sole energy-storing species. The values obtained in this work are collected in Table 2 and are in agreement with those obtained by the deconvolution method and also with that reported by Schmidt et al. [9] ($E_T = 182$ kJ mol^{-1}). However, they are significantly lower than that reported by Oliveros et al. [15] from 77 K phosphorescence spectroscopy in methylcyclohexane ($E_T = 220$ kJ mol^{-1}).

4. Conclusions

Four aromatic ketones were explored as possible universal standards for $O_2(^1\Delta_g)$ photosensitization. PN and its more water-soluble 2-sulphonic acid derivative PNS emerge as the only sensitizers that preserve their high ϕ_Δ values in all solvents assayed. The absolute ϕ_Δ values for this compound were determined in several solvents with the LIOAC technique, using the maximum amplitude and deconvolution methods. The former yields more precise calorimetric results, but its use is restricted to systems in which oxygen quenching of the triplet sensitizer occurs in the "fast" time regime, i.e. $\tau_T < \tau'_a/5$. The latter is free from such restrictions and provides E_T, ϕ_Δ and τ_T data in a single experiment, albeit with larger uncertainties. The description of PN photophysics was completed by including the rate constants for triplet quenching by oxygen and the triplet energies in several solvents. Using the LIOAC ϕ_Δ values for PN, the absolute ϕ_Δ values for the other ketones can be calculated from the relative values in Table 1. The resulting recommended values are collected in Table 3.

Acknowledgements

We are indebted to Dr. C. Viappiani for allowing us to use his deconvolution program. Fruitful discussions with Professor S.E. Braslavsky were greatly appreciated. C.M. thanks the "Fundacion Patronato del Instituto Quimico de Sarria"

for a fellowship. This work was supported by grant QFN94-4613-C02-1 from the CICYT and the Generalitat de Catalunya.

References

[1] F. Wilkinson, W.P. Helman and A.B. Ross, *J. Phys. Chem. Ref. Data, 22* (1993) 113.
[2] R.D. Scurlock and P.R. Ogilby, *J. Phys. Chem., 91* (1987) 4599.
[3] R.D. Scurlock, S. Nonell, S.E. Braslavsky and P.R. Ogilby, *J. Phys. Chem., 99* (1995) 3521.
[4] G. Rossbroich, N.A. Garcia and S.E. Braslavsky, *J. Photochem., 31* (1985) 35.
[5] K. Heihoff, R.W. Redmond, S.E. Braslavsky, M. Rougée, C. Salet, A. Favre and R.V. Bensasson, *Photochem. Photobiol., 51* (1990) 635.
[6] R.R. Hung and J.J. Grabowski, *J. Phys. Chem., 95* (1991) 6073.
[7] R.W. Redmond, *Photochem. Photobiol., 54* (1991) 547.
[8] S.E. Braslavsky and G.E. Heibel, *Chem. Rev., 92* (1992) 1381.
[9] R. Schmidt, C. Tanielian, R. Dunsbach and C. Wolff, *J. Photochem. Photobiol. A: Chem., 79* (1994) 11.
[10] M. Terazima, N. Hirota, H. Shinoshara and Y. Saito, *J. Phys. Chem., 95* (1991) 9080.
[11] R.W. Redmond, K. Heihoff, S.E. Braslavsky and T.G. Truscott, *Photochem. Photobiol., 45* (1987) 209.
[12] A.P. Darmanyan and C.S. Foote, *J. Phys. Chem., 97* (1993) 4573.
[13] C. Grewer and H.-D. Brauer, *J. Phys. Chem., 97* (1993) 5001.
[14] T.A. Jenny and N.J. Turro, *Tetrahedron Lett., 23* (1982) 2923.
[15] E. Oliveros, P.S. Murasecco, T.A. Saghafi, A.M. Braun and H.J. Hansen, *Helv. Chim. Acta, 74* (1991) 79.
[16] S. Nonell, M. González and F.R. Trull, *Afinidad, 50* (1993) 445.
[17] A.A. Gorman, I. Hamblett, C. Lambert, A.L. Prescott, M.A.J. Rodgers and H.M. Spence, *J. Am. Chem. Soc., 109* (1987) 3091.
[18] A.A. Gorman, A.A. Krasnovsky and M.A.J. Rodgers, *J. Phys. Chem., 95* (1991) 598.
[19] S.L. Logunov and M.A.J. Rodgers, *J. Phys. Chem., 97* (1993) 5643.
[20] F. Wilkinson, D.J. McGarvey and A.F. Olea, *J. Phys. Chem., 98* (1994) 3762.
[21] J.C. Scaiano, *CRC Handbook of Organic Photochemistry*, CRC Press, Boca Raton, FL, 1989.
[22] S.L. Murov, I. Carmichael and G.L. Hug, *Handbook of Photochemistry*, Marcel Dekker, New York, 1993.
[23] D.F. Eaton, *Pure Appl. Chem., 60* (1988) 1107.
[24] G. Valduga, S. Nonell, E. Reddi, G. Jori and S.E. Braslavsky, *Photochem. Photobiol., 48* (1988) 1.
[25] S. Nonell, S.E. Braslavsky and K. Schaffner, *Photochem. Photobiol., 51* (1990) 551.
[26] C.K.N. Patel and A.C. Tam, *Rev. Mod. Phys., 53* (1981) 517.
[27] L.J. Rothberg, J.D. Simon, M. Bernstein and K.S. Peters, *J. Am. Chem. Soc., 105* (1983) 3464.
[28] D.I. Schuster, G.E. Heibel, R.A. Caldwell and W. Kang, *Photochem. Photobiol., 52* (1990) 645.
[29] P.R. Crippa, A. Vecli and C. Viappiani, *J. Photochem. Photobiol. B: Biol., 24* (1994) 3.
[30] T.J. Burkey, M. Majewski and D. Griller, *J. Am. Chem. Soc., 108* (1986) 2218.
[31] K.S. Peters, T. Watson and K. Marr, *Annu. Rev. Biophys. Chem., 20* (1991) 343.
[32] K. Marr and K.S. Peters, *Biochemistry, 30* (1991) 1254.
[33] R.R. Hung and J.J. Grabowski, *J. Am. Chem. Soc., 114* (1992) 351.
[34] P.J. Schulenberg, M. Rohr, W. Gärtner and S.E. Braslavsky, *Biophys. J., 66* (1994) 838.
[35] S.E. Braslavsky and K. Heihoff, in J.C. Scaiano (ed.), *Handbook of Organic Photochemistry*, CRC Press, Boca Raton, FL, 1989, p. 327.
[36] J. Feitelson and D.C. Mauzerall, *J. Phys. Chem., 97* (1993) 8410.
[37] J.E. Rudzki, J.L. Goodman and K.S. Peters, *J. Am. Chem. Soc., 107* (1985) 7849.
[38] L.A. Melton, T. Ni and Q. Lu, *Rev. Sci. Instrum., 60* (1989) 3217.
[39] J. Rudzki-Small, L.J. Libertini and E.W. Small, *Biophys. Chem., 42* (1992) 29.
[40] M. Terazima and T. Azumi, *Bull. Chem. Soc. Jpn., 63* (1990) 741.
[41] N.S. Allen, *Polym. Photochem., 3* (1983) 167.
[42] P. Van Haver, L. Viaene, M. Van der Auweraer and F.C. De Schryver, *J. Photochem. Photobiol. A: Chem., 63* (1992) 265.
[43] A.A. Lamola and G.S. Hammond, *J. Chem. Phys., 43* (1965) 2129.
[44] J.B. Guttenplan and S.G. Cohen, *Tetrahedron Lett., 26* (1969) 2125.
[45] R.A. Caldwell and R.P. Gajewski, *J. Am. Chem. Soc., 93* (1971) 532.
[46] J.C. Scaiano, *J. Am. Chem. Soc., 102* (1980) 7747.
[47] R.D. Scurlock and P.R. Ogilby, *J. Phys. Chem., 93* (1989) 5493.
[48] A.P. Darmanyan and C.S. Foote, *J. Phys. Chem., 97* (1993) 5032.
[49] R.W. Redmond and S.E. Braslavsky, *Chem. Phys. Lett., 148* (1988) 523.
[50] O.L.J. Gijzeman, F. Kaufman and G. Porter, *J. Chem. Soc., Faraday Trans. 2, 69* (1973) 708.
[51] O.L.J. Gijzeman and F. Kaufman, *J. Chem. Soc., Faraday Trans. 2, 69* (1973) 721.